

The Relationship between Surface Corneal Topography and Stromal Collagen Organisation in Normal and Keratoconus Corneas

S Hayes¹, C Boote¹, Y Huang² and K M Meek¹

1. Structural Biophysics Research Group, School of Optometry and Vision Sciences, Cardiff University, Redwood Building, King Edward VII Avenue, Cardiff CF10 3NB, UK

2. Department of Ophthalmology, Great Wall Hospital of PLA, 28 Fuxing Road, Beijing P.R. China

Abstract

A specific arrangement of collagen provides the cornea with its strength, shape and transparency. As a result, abnormalities in the structural organisation of stromal collagen have been implicated in several corneal diseases, such as keratoconus. The aim of this study is to examine the relationship between corneal structure and specific keratoconus shape changes to improve our understanding of the mechanism by which the disease progresses. High-angle X-ray fibre diffraction was used to map the preferred orientation and distribution of fibrillar collagen in a normal cornea and two excised keratoconus corneal buttons. The X-ray diffraction data were examined alongside videokeratographic images of the same corneas taken prior to surgery. Abnormalities in collagen orientation and mass distribution were seen in both of the keratoconus corneal buttons. A relationship appeared to exist between the size and shape of the cone and the extent of structural alterations in the stroma of keratoconus corneal buttons. The results are consistent with a theoretical mechanism of keratoconus progression which involves enzyme action and inter-fibrillar and inter-lamellar slippage, causing a loss of some tissue mass and a redistribution of the remaining tissue mass within the corneal button region.

Keywords: Cornea, keratoconus, X-ray scattering

Introduction

The cornea, which is a tough, transparent tissue covering the front of the eye, acts as the main refractive component of the ocular system; its precise curvature determines the quality of the image formed on the retina. The stroma forms 90% of the cornea and is composed primarily of water and Type I collagen.

Within the stroma, parallel collagen fibrils are arranged in layers (lamellae) which travel in all directions within the

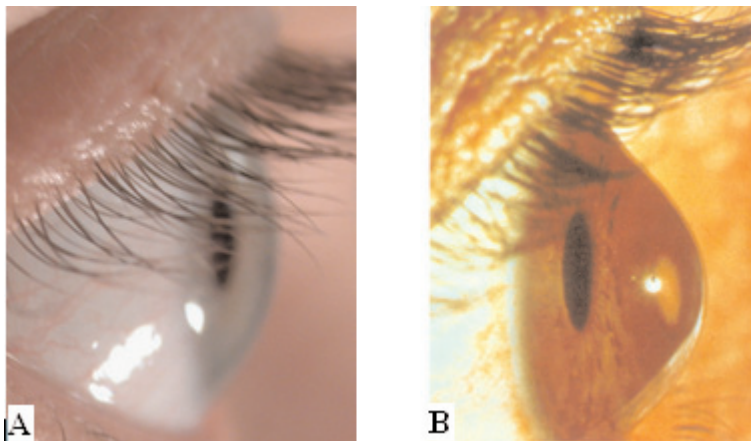
plane of the cornea but predominantly in the superior-inferior and nasal-temporal directions.

The specific arrangement of collagen provides the cornea with its shape, transparency and strength [1, 2]. As a result of this, abnormalities in collagen organisation have been implicated in several corneal diseases, one of which is keratoconus, a condition that is characterised by a progressive thinning and steepening of the cornea, resulting in severe, irregular astigmatism (Figure 1B).

Keratoconus affects between 4 and 200 people per 100,000 [3], and is the second most common cause of corneal transplant surgery in the UK [4].

The advent of computer-assisted corneal topography analysis (videokeratography) in recent years has greatly facilitated the early diagnosis and monitoring of keratoconus, by providing the clinician with information about the precise shape of the cornea in the form of a colour coded contour map of corneal dioptric power.

Figure 1. The side profile of a normal cornea (A) and a keratoconus cornea (B).



Once diagnosed, the majority of cases may be successfully treated through the use of glasses and hard contact lenses. However, in 10-20% of keratoconus patients, severe corneal scarring at the apex of the cone results in a permanent decrease in visual acuity that can only be restored by means of a corneal transplant.

The present study examines the interesting relationship between corneal structure and shape by examining X-ray diffraction derived information about the arrangement and distribution of collagen in normal and keratoconus corneas alongside videokeratographic images of the same corneas.

Methods

Tissue samples

Two unscarred keratoconus corneal buttons of 6.5 mm diameter were obtained at the time of penetrating keratoplasty from Great Wall Hospital (Beijing, Japan) with the patients' consent. Keratoconus button 1, which was from the left eye of a 17-year-old male, had a maximum corneal dioptric power of 72.79D. Keratoconus button 2, which was from the left eye of a 26-year-old male, had a maximum corneal dioptric power of 81.10D. Both buttons were tagged at the 12 o'clock position with a nylon suture before being preserved in 2.5% formalin. A normal human eyeball (removed within 3 hours post mortem) was also tagged at the 12 o'clock position and stored in 2.5% formalin. Immediately prior to data collection the cornea with a 2mm scleral rim was carefully dissected from the normal human globe using a scalpel.

Videokeratography

Prior to surgery, videokeratographic images of corneal surface dioptric power were recorded using an EyeSys topography system (EyeSys Vision, Texas, USA). A grid overlay of 1 x 1 mm squares was superimposed onto the topography map to highlight the position, size and shape of the cone. In the case of the normal post mortem eyeball, videokeratography was performed within 2 hours after enucleation. The same colour and dioptric interval scale was used for each map, whereby warm colours represent the regions of highest dioptric power (the steepest regions) and cold colours indicate the areas of lowest dioptric power (flatter regions).

X-ray diffraction data collection

All X-ray diffraction data were collected on Station 14.1 at Daresbury Synchrotron Radiation Source (Warrington, UK), using a 0.2 x 0.2 mm beam with a wavelength of 0.1488 nm. The samples were wrapped tightly in cling-film (to prevent tissue dehydration during data collection) before being placed (in their correct orientation) into an airtight sample holder enclosed between two sheets of Mylar (Dupont-Teijin, UK). The sample holder was then carefully secured onto a computer-operated translation stage with the most anterior side of the cornea facing the

X-ray beam. High-angle X-ray diffraction images were collected over the entire sample at regular intervals of 0.4 mm in the case of the normal cornea with scleral rim and 0.5 mm for each of the keratoconus buttons. The X-ray exposure time of 75 seconds per image used for the normal cornea was increased to 180 seconds for the thinner keratoconus corneal buttons in order to maximise the signal to noise ratio. X-ray diffraction images (Figure 2A) were recorded on a Quantum 4R CCD detector (ADSC, Poway, CA) placed 150 mm behind the sample.

X-ray diffraction data analysis

The angular distribution of scatter intensity around the intermolecular reflection (Figure 2A) was measured to form a 0-360° distribution pattern (Figure 2B) using Optimus 6.5 (Media Cybernetics, UK) image analysis software and Excel (Microsoft, UK). To take into account variations in beam intensity and exposure time between samples, the intensity profile for each image was normalised against the average X-ray intensity (recorded by an ion chamber at the time of exposure) multiplied by the exposure time. The intensity profile was then folded to improve the signal to noise ratio; this was possible without the loss of any data, due to the centro-symmetric nature of X-ray fibre diffraction patterns. At this stage, the total area under the intensity profile (i.e. the total scatter) is proportional to the total mass of fibrillar collagen in the path of the X-ray beam (Figure 2B). This can be divided into two components; isotropic scatter arising from a background of collagen fibrils equally disposed in all directions within the plane of the cornea and aligned scatter from fibrils that adopt a preferred orientation [5]. Removal of the isotropic scatter leaves only the scatter from preferentially aligned lamellae, which we will refer to as 'aligned collagen' (Figure 2C).

The area under each intensity profile (Figures 2B and 2C) was summed to produce a numeric value of scatter intensity for both total collagen mass and aligned collagen mass. The scatter intensity from aligned collagen as a proportion of the total collagen scatter was calculated to form a ratio (index of orientation), whereby an index of 1 indicates that all of the collagen at that particular point in the tissue is preferentially aligned and an index of 0 means that the collagen is distributed equally in all directions within the plane of the cornea. Two-dimensional contour maps showing the distribution of total collagen scatter and the index of orientation were formed by plotting each calculated intensity value/index onto a grid relating to corneal position. On the assumption that the keratoconus buttons and the normal cornea were similarly hydrated, the scatter distribution contour plots represent the relative distribution of collagen mass within each sample. By presenting aligned collagen mass as an index of orientation, the reduced stromal thickness of the keratoconus corneas is taken into account, thereby highlighting any differences in aligned collagen mass distribution between the normal and keratoconus corneas.

To show the preferred orientation of aligned collagen molecules at a specific point in the tissue, the intensity profile of aligned collagen scatter was shifted by 90° (to account for the fact that the high-angle equatorial reflection appears at right angles to the fibril axis) and then converted to a vector plot (Figure 2D) [5]. The distance from the centre of a vector plot to the edge, at any given angle, represents the intensity of aligned collagen scatter from collagen molecules oriented in that particular direction. As the collagen molecules are aligned roughly parallel to each other and the fibril axis, the orientation of the molecules can be said to reasonably represent the direction of the collagen fibrils at that position within the corneal stroma. The individual vector plots were compiled onto a grid relating to corneal position to form a 'vector plot map', showing the preferred orientation of aligned collagen across each sample.

Results

Figure 3 shows the index of orientation in the central 10 mm of a normal right cornea. The index of orientation increases in all four quadrants of the peripheral cornea,

but most prominently in the superior-nasal and inferior-temporal quadrants. Within the central 6.4 mm region (highlighted by a dashed blue line in Figure 3), the increase in the index of orientation is seen only in the superior-nasal and inferior-temporal quadrants. As a non-superimposable mirror symmetry of collagen mass distribution has been shown to exist between the normal left and right cornea [7], it is possible for the purposes of this study to compare the distribution of collagen mass in two left 6.5 mm keratoconus buttons to the distribution of collagen mass in the central 6.4mm region of a normal right cornea (Figure 4).

Videokeratography

Figure 4 (A-C) shows the corneal surface dioptric power of the normal cornea and two keratoconus corneas. In contrast to the normal cornea, which has a maximum dioptric power of 45.69D (Figure 4A), both keratoconus corneas have regions of very high dioptric power (66.39D in keratoconus button 1 and 69.33D in keratoconus button 2) which highlight the position, size and the shape of the cone (Figure 4B and C). Keratoconus button 1 has a large centrally positioned round cone which measures 5.08mm

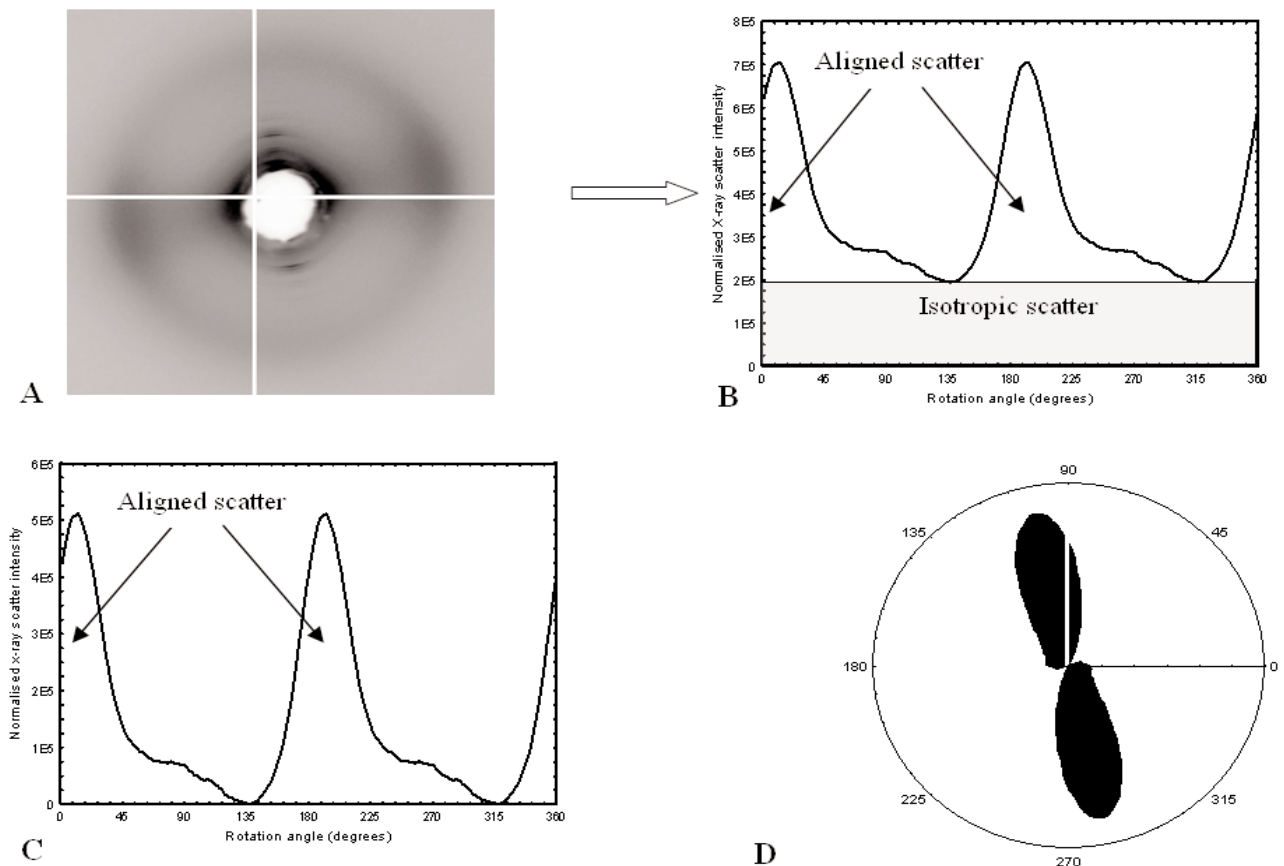


Figure 2. A high angle X-ray scattering pattern from corneal collagen (A). The profile of total collagen scattering intensity (from both isotropic and preferentially aligned collagen) (B) and preferentially aligned collagen scatter only (C), are shown as a function of angular position around the X-ray scatter pattern. The profile of aligned collagen scatter intensity is converted to a vector plot (D), taking into account the fact that X-rays are scattered at right-angles to the fibril axis. The distance from the centre of a vector plot in any given direction is representative of the amount of collagen fibrils preferentially orientated in that particular direction.

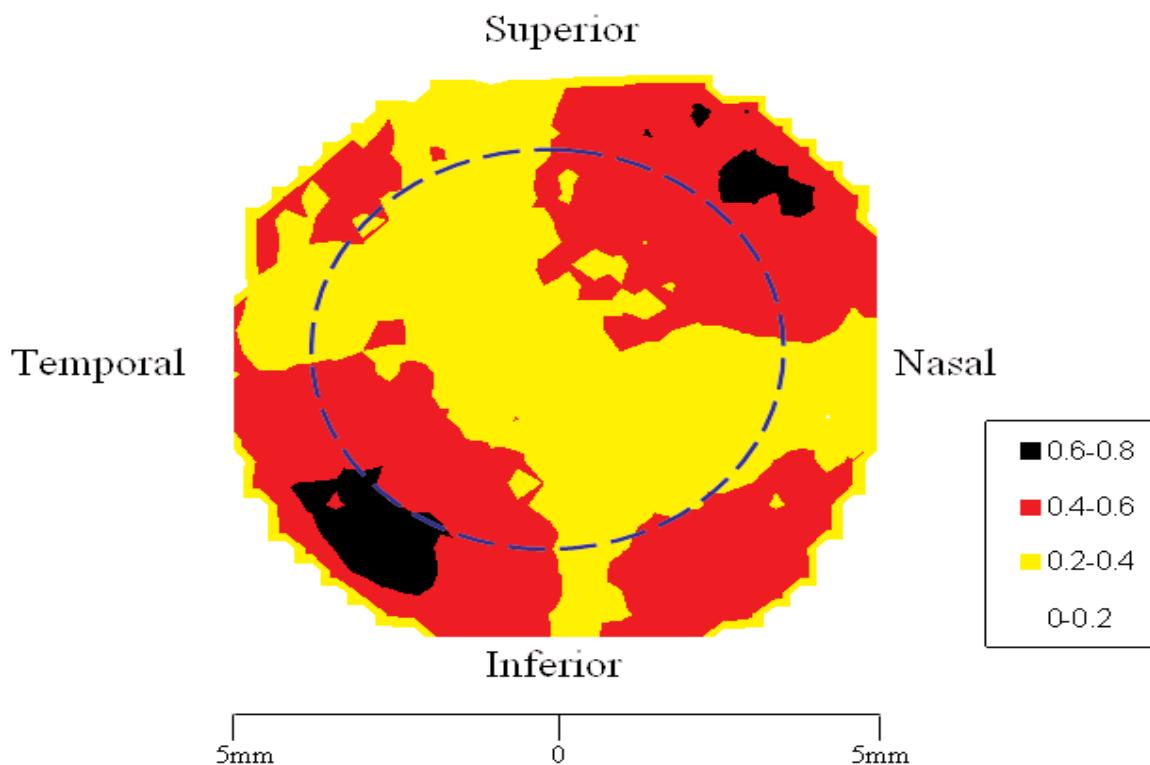


Figure 3. A contour map showing the index of orientation (aligned/total collagen mass) in the central 10mm of a normal right human cornea. The index of orientation increases in all four quadrants of the peripheral cornea, but predominantly in the superior-nasal and inferior-temporal quadrants. The central 6.4 mm region is highlighted by a blue dashed line; this region will be used for comparison with keratoconus buttons 1 and 2.

in radius (when shown as a 2D projection) and keratoconus button 2 has a smaller inferior-temporally located oval cone of 4.87mm radius.

Preferred collagen orientation

In Figure 4 (D-F) vector plot maps show the preferred orientation of aligned collagen in the central 6.4 mm region of the normal cornea and in the central 6.5 mm region of keratoconus buttons 1 and 2. In the normal cornea more aligned collagen fibrils lie in the superior-inferior and nasal-temporal directions than in any other which gives rise to the characteristic cross shaped vector plots seen in previous studies of normal human corneas [6, 8]. Towards the edge of the 6.4 mm region, the preferred orthogonal orientation is gradually 'swamped' by additional aligned collagen lying tangentially to the edge of the cornea (Figure 4D).

The normal preferred orientation of collagen in the central cornea is lost to varying extents in both of the keratoconus corneal buttons (Figure 4E and F). In keratoconus button 1, which exhibits a large round cone (Figure 4B) the normal orthogonal orientation is lost throughout most of the 6.5 mm button (Figure 4E). In the case of keratoconus 2, which has an oval-shaped cone (Figure 4C), the preferred orientation of aligned collagen is only altered at the apex of the cone (Figure 4F). In both cases, the disruption to normal preferred collagen orientation is great-

est at the apex of the cone and decreases with distance from the apex.

Total collagen mass distribution

Contour plots showing the distribution of total collagen mass in the normal right cornea and the two left keratoconus buttons are shown in Figure 4 (G-I). When shown on the same intensity scale as the keratoconus corneal buttons, the distribution of collagen mass in the normal cornea appears to be fairly uniform across the central 6.4 mm region. In both keratoconus buttons the total collagen mass is lower than normal within the region of the cone. This is as one might expect since maximal stromal thinning is known to occur within the cone region of keratoconus corneas.

Index of orientation

The index of orientation in the central 6.4 mm of the normal right cornea is highest in the superior-nasal and inferior-temporal quadrants where between 40 and 60% of the total collagen is preferentially aligned (Figure 4J). As mentioned previously, the increase in the index of orientation occurs predominantly in the superior-nasal and inferior-temporal quadrants of both left and right corneas [7]. However, within the central 6.5 mm of keratoconus button 1 (which has a round, centrally located cone; Figure 4B) the index of orientation increases to a similar extent in all four quadrants (Figure 4K).

In the central 6.5mm region of keratoconus button 2 (which has an oval, inferior-temporally located cone) (Figure 4C), the index of orientation increases only in the superior-nasal and inferior-temporal quadrants; this is as one might expect for a normal left cornea based on the findings of Boote and colleagues [7]. However, in the case of keratoconus button 2, the index of orientation is higher than normal and occurs well within the main optical zone of the cornea (Figure 4L).

Discussion

There are at present two main theories regarding the mechanism of stromal thinning in the cone region of keratoconus corneas; one is a loss of collagen mass through tissue degradation [9], and the other is a redistribution of collagen mass by means of inter-fibrillar or inter-lamellar slippage [10]. Despite much research, the exact mechanism by which the cornea thins and steepens in keratoconus is still unknown. However, for the first time, we are able to link specific keratoconus shape changes to structural alterations within the stroma by examining X-ray diffraction data alongside videokeratographic images of surface corneal power.

As collagen has greatest tensile strength along its fibril axis and is preferentially orientated in most tissues in the direction of greatest stress [11], this has prompted suggestions that the preferred orthogonal orientation of fibrils in the superior-inferior and nasal-temporal directions of the normal cornea (Figure 4D) may resist the stress exerted by the extra-ocular muscles and so prevent tissue distortion during eye movement [6, 8, 12].

In both keratoconus corneas, the normal orthogonal preferred orientation of collagen was lost within the cone region and in the case of keratoconus button 1 (which had the largest cone); a disturbed arrangement of collagen was also observed throughout the remainder of the 6.5 mm button. Consistent with previous studies [3, 12-15], the most striking changes in collagen orientation were observed at the apex of the cone and gradually decreased with distance from the apex. As the amount of collagen alignment in the superior-inferior and nasal-temporal directions of the normal cornea is highest in the posterior stroma [16], these findings provide evidence that major structural alterations occur in the posterior stroma of advanced keratoconus corneas.

The observed decrease in collagen mass in the cone region of both keratoconus corneas supports both clinical and experimental findings of maximal thinning in this region [17-19]. It must be remembered, however, that although the maps of collagen mass distribution indicate a loss of collagen mass from the central 6.5mm region of both keratoconus corneas, this does not necessarily mean that there is a loss of collagen mass from the entire cornea; the possibility remains that collagen mass is not

lost but simply redistributed to a location outside the button region.

The current findings in fact provide evidence of a loss of total collagen mass from the central 6.5mm region and also a redistribution of the remaining collagen mass within the button region. The latter is evident when the distribution of aligned collagen mass is examined as an index of orientation (relative to the total collagen mass). In the normal cornea, there is a large increase in the index of orientation in the superior-nasal and inferior-temporal quadrants (at a distance of 1.6 mm from the centre of the cornea) and also to a much lesser extent in the superior-temporal and inferior-nasal quadrants (Figure 3). It has been suggested that the increased index of orientation in the four quadrants of the normal cornea, may be due to the presence of additional aligned collagen that traverses the peripheral cornea and facilitates the flattening of the cornea prior to the limbus [6, 15]. However, both keratoconus corneal buttons differed from the normal cornea (and from each other) in terms of aligned collagen mass distribution. In the case of keratoconus button 1, which had a large, round, centrally located cone, the index of orientation increased in all four quadrants, whereas in keratoconus button 2, which had a smaller oval, inferior-temporally located, cone, the index of orientation in the 6.5 mm button region increased dramatically in the superior-nasal and inferior-temporal quadrants and was twice as high as normal within the main optical zone of the cornea.

The findings presented in this study have provided evidence that changes in the orientation and distribution of tissue mass in keratoconus corneas are related to the specific shape, size and location of the cone. The observed disruption to collagen orientation and mass distribution support a mechanism of tissue thinning in keratoconus corneas that involves inter-fibrillar or inter-lamellae slippage and tissue redistribution. Irrespective of the original cause of thinning in keratoconus, the structural changes identified in this study would likely further accelerate the progression of the disease as the biomechanical stability of the cornea is compromised.

Acknowledgements

The authors wish to thank Dr Mike MacDonald and the staff at the UK Synchrotron X-ray Source (Daresbury, UK) for help with data collection. This study received support from the Medical Research Council (#G0001033) and the Council for the Central Laboratory of Research Councils.

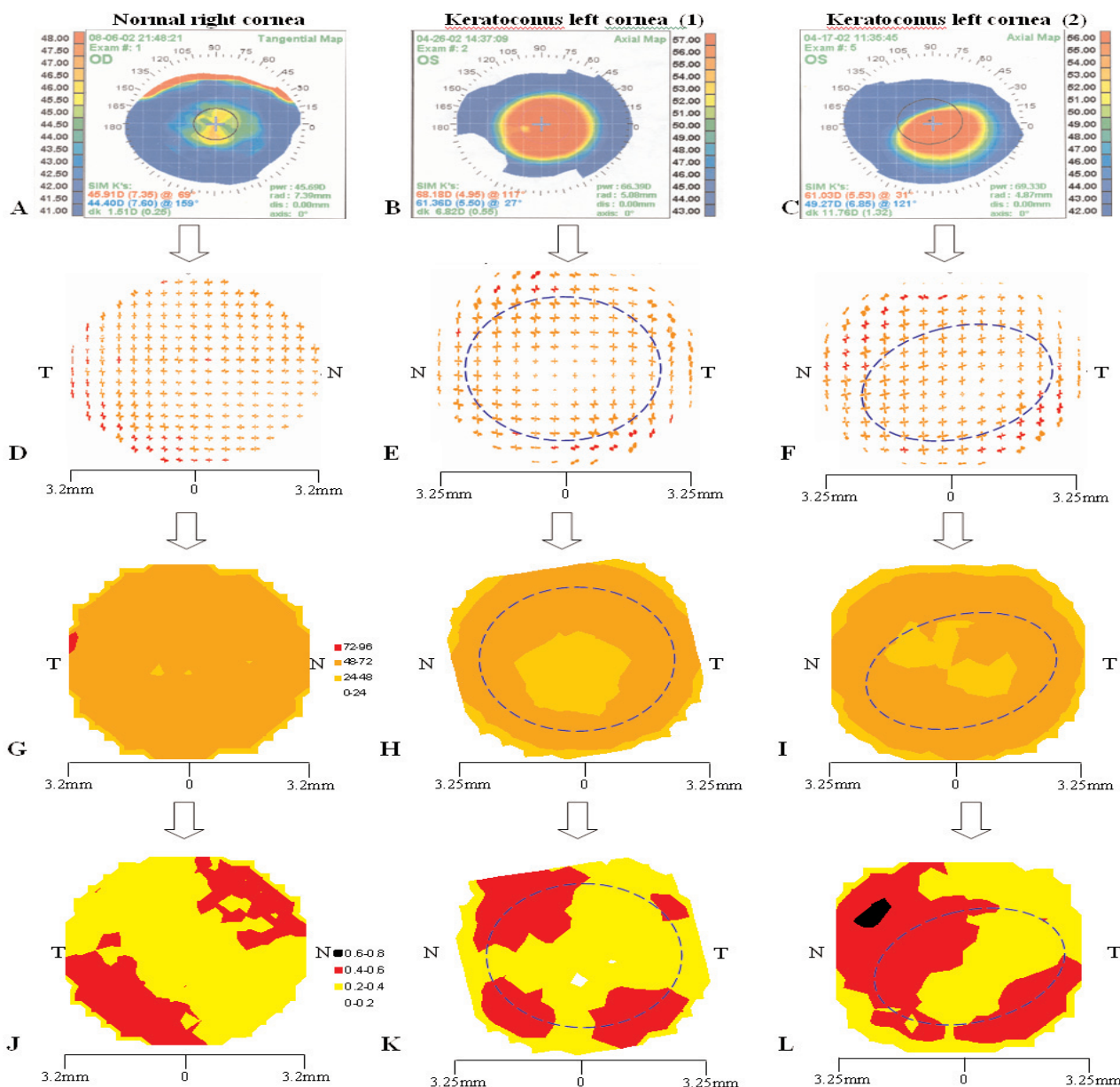


Figure 4 Videokeratography images of a normal right cornea (A) and two left keratoconus corneas (B and C). Vector plot maps show the preferred orientation of aligned collagen in the central 6.4 mm region of the same normal right cornea (D) and the same two left 6.5 mm keratoconus corneal buttons (1 (E) and 2 (F)). Due to variations in the intensity of aligned X-ray scatter across an individual cornea (caused by variations in the amount of aligned collagen), red polar plots have been scaled down by a factor of 1.5 so that all of the vector plots can be viewed on the same map. The distribution of fibrillar collagen mass (G-I) and the index of orientation (J-L) in the same regions of the normal cornea and the two keratoconus corneal buttons are also shown. In the case of the keratoconus buttons, the region of highest dioptric power is highlighted (by a blue dashed line) in each of their respective contour and vector plot maps, to indicate the size and shape of the cone.

References

- [1] Maurice, D.M. 1957. The structure and transparency of the cornea. *Journal of Physiology* 136, 263-286.
- [2] Maurice, D.M. 1988. Mechanics of the cornea. In: Cavanagh, H.D. ed./eds. *The cornea: Transactions of the world congress on the cornea III*. New York: Raven Press Ltd. pp. 187-192.
- [3] Krachmer, J.H., Feder, R.S. and Belin, M.W. 1984. Keratoconus and related non-inflammatory corneal thinning disorders. *Survey of Ophthalmology* 28, 293-322.

- [4] Al-Yousuf, N., Mavrikakis, I., Mavrikakis, E. et al. 2004. Penetrating keratoplasty: Indications over a 10 year period. *British Journal of Ophthalmology* 88, 998-1001.
- [5] Daxer, A. and Fratzl, P. 1997. Collagen fibril orientation in the human cornea and its implications in keratoconus. *Investigative Ophthalmology and Visual Science* 38, 121-129.
- [6] Aghamohamadzadeh, H., Newton, R.H. and Meek, K.M. 2004. X-ray scattering used to map the preferred collagen orientation in the human cornea and limbus. *Structure* 12, 249-256.
- [7] Boote, C., Hayes, S., Abahussin, M. and Meek, K.M. 2005. Mapping the structure of the human cornea: mirror symmetry in collagen organisation between left and right eyes. *Investigative Ophthalmology and Visual Science*. In Press.
- [8] Meek, K.M. and Newton, R.H. 1999. Organization of collagen fibrils in the corneal stroma in relation to mechanical properties and surgical practice. *Journal of Refractive Surgery* 15, 695-699.
- [9] Kenney, M.C. and Brown, D.J. 2003. The Cascade Hypothesis of Keratoconus. *Contact Lens and Anterior Eye* 26, 139-146
- [10] Polack, F.M. 1976. Contributions of electron microscopy to the study of corneal pathology. *Survey of Ophthalmology* 20, 375-414.
- [11] Ottani, V., Raspanti, M. and Ruggeri, A. 2001. Collagen structure and functional implications: A review. *Micron* 32, 251-260.
- [12] Daxer, A. and Fratzl, P. 1997. Collagen fibril orientation in the human corneal stroma and its implications in keratoconus. *Investigative Ophthalmology and Visual Science* 38, 121-129.
- [13] Radner, W., Zehetmayer, M., Skorpik, C. et al. 1998. Altered organization of collagen in the apex of keratoconus corneas. *Ophthalmic Research* 30, 327-332.
- [14] Sawaguchi, S., Fukuchi, T., Abe, H. et al. 1998. Three dimensional electron microscopic study of keratoconus. *Archives of Ophthalmology* 116, 62-98.
- [15] Meek, K.M., Tuft, S.J., Huang, Y. et al. 2005. Changes in collagen orientation and distribution in keratoconus corneas. *Investigative Ophthalmology & Visual Science* 46, 1948-1956.
- [16] Meek, K., Blamires, T., Elliot, G. et al. 1987. The organisation of collagen fibrils in the human corneal stroma: A synchrotron x-ray diffraction study. *Current Eye Research* 6, 841-846.
- [17] Mandell, R. and Polse, K.A. 1969. Keratoconus: Spatial variation of corneal thickness as a diagnostic test. *Archives of Ophthalmology* 82, 182-188.
- [18] Auffarth, G.U., Wang, L. and Volcker, H.E. 2000. Keratoconus evaluation using the orbscan topography system. *Journal of Cataract Refractive Surgery* 26, 222-228.
- [19] Liu, Z., Zhang, M., Chen, J. et al. 2002. Corneal topography and thickness in keratoconus [article in chinese]. *Chung Hua Yen Ko Tsa Chih* 38, 740-743.